Articles

Ethylene−Norbornene Copolymers by C_s-Symmetric Metallocenes: Determination of the Copolymerization Parameters and Mechanistic Considerations on the Basis of Tetrad Analysis

Incoronata Tritto,* Laura Boggioni, Cristina Zampa, and Dino R. Ferro

Istituto per lo Studio delle Macromolecole, Consiglio Nazionale delle Ricerche Via E. Bassini 15, I-20133 Milano, Italy

Received July 29, 2005; Revised Manuscript Received September 26, 2005

ABSTRACT: The copolymerization of ethylene and norbornene by catalytic systems composed of *i*-Pr-[(Cp)(Flu)]$ZrCl_2$ (**1**) and methylaluminoxane was investigated. Ethylene−norbornene (E−N) copolymers with 40.2 mol % of norbornene are highly alternating (NENE 50 mol %) and contain a significant amount of *racemic* ENNE (8 mol %) and no ENNN sequences. The microstructural analysis by ^{13}C NMR of such copolymers was completely obtained at the tetrad level by a methodology that exploits all the peak areas of the spectra and accounts for the stoichoimetric requirements of the copolymer chain. The analysis at the tetrad level allowed us to test the statistical model best describing E−N copolymerization with C_s-symmetric catalyst **1** and to study the polymerization mechanism. The root-mean-square deviations between experimental and calculated tetrads demonstrate that the first-order Markov model is sufficient to describe the microstructure of E−N copolymers with **1**. It is concluded that in E−N copolymerizations with this catalyst both N and E are inserted according to a Cossee's migratory insertion, and backskips of the copolymer chain to its original position occur, causing the formation of both *meso* and *racemic* NEN sequences. The probability of chain backskip is relatively high with respect to that observed in syndiotactic propylene polymerization under the same polymerization conditions. This effect seems to be due to norbornene strong coordinating ability which can influence the competition between site epimerization and chain propagation.

Introduction

The synthesis of poly-α-olefins by *ansa*-metallocene-based catalysts is one of the most efficient stereoselective catalytic reactions.[1] The stereoselectivity of these systems strongly depends on the metallocene symmetry and ligand type. The first metallocene able to produce highly syndiotactic polypropylene was the C_s-symmetric R_2C[(Cp)(9-Flu)]$ZrCl_2$ (**1**; R = Me; Cp = C_5H_4; Flu = fluorenyl) (Chart 1).[2] The analysis of the stereochemistry of poly-α-olefins has proven to provide new insights into the mechanistic details of catalytic olefin polymerization. The pathway for the syndiospecific propylene enchainment has been explained in terms of chain migratory insertion and considered one of the evidences for Cossee's[3] alternating mechanism. Since the discovery of these catalysts, many authors have discussed about the origin of their syndiospecificity.[4] The current view can be summarized as following: (i) C_s-symmetric metallocene **1** possesses one bulky substituent (fluorenyl), which directs the growing polymer chain toward the less hindered cyclopentadienyl side; (ii) the fluorenyl presents an empty space in the central region wide enough to accommodate the methyl of propylene in trans with respect to the polymer chain; (iii) the growing polymer chain and the incoming monomer alternate their coordination to the two enantiotopic sites, determining a migratory type of insertion (Figure 1). The presence of stereoerrors such as *rrrmmrrrr* is consistent with site control (Figure 2); the presence of a variable amount of *rrrmrrrr* indicates occasional skipped insertions (Figure 3).

Chart 1. Metallocene under Investigation *i*-Pr(Cp)(Flu)$ZrCl_2$ (1)

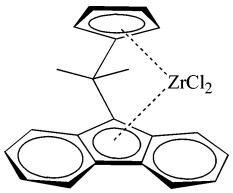

These catalysts are known to be able to catalyze the polymerization of cyclic olefins and ethylene (E)−norbornene (N) copolymerization, which provides one of the new families of olefinic copolymers made available thanks to the advent of metallocene catalysts.[5,6] Advances on norbornene copolymerization with early transition metal catalysts have been recently reviewed.[7] Our continuing effort to elucidate the E−N copolymer microstructure through ^{13}C NMR analysis has provided novel signal assignments of the complex spectra of these copolymers, a description of the copolymer microstructure up to the pentad level of details, and insights into the copolymerization mechanism.[8−15] As part of this interest, we have recently reported on the microstruc-

* Corresponding author. E-mail: i.tritto@ismac.cnr.it.

10.1021/ma051682j CCC: $30.25
Published on Web 10/26/2005

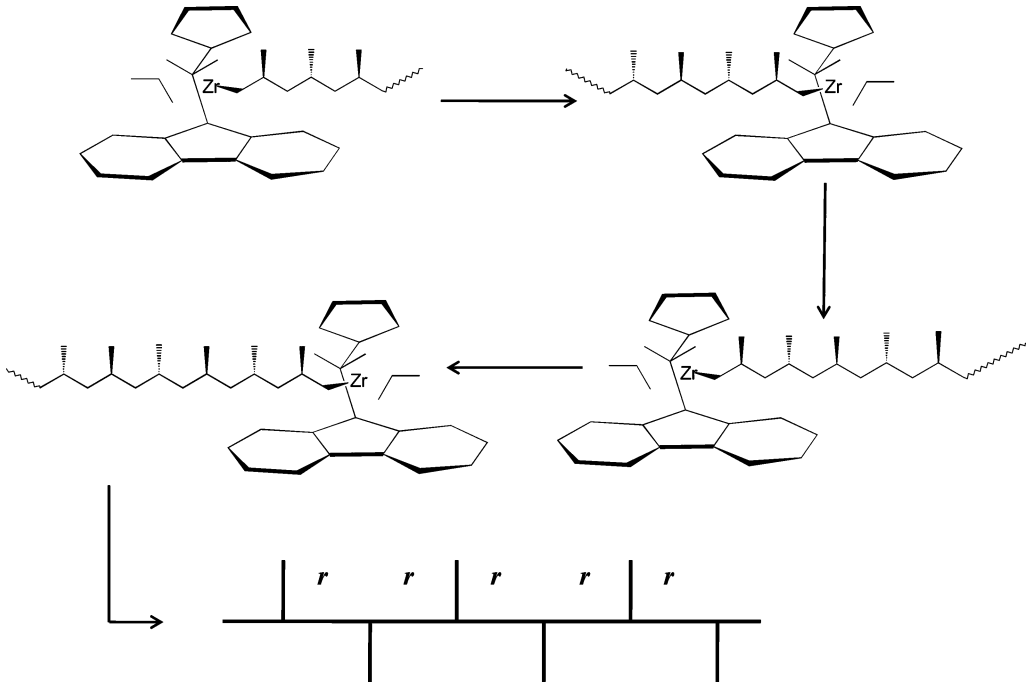

Figure 1. Propylene polymerization with C_s-symmetric catalysts: Cossee's alternating mechanism.

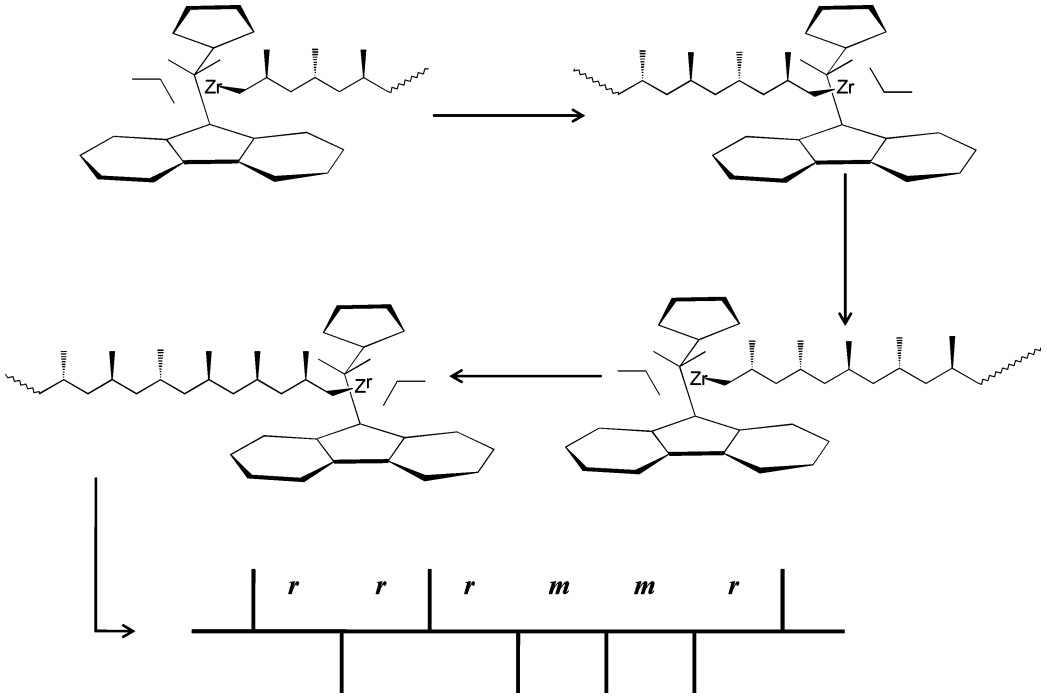

Figure 2. Syndiotactic polypropylene by site control with C_s-symmetric metallocenes: isolated stereoerrors.

tural analysis of the NMR spectra of alternating isotactic E−N copolymers synthesized with the two C_1-symmetric metallocene-based catalysts *i*-Pr(3-Pr^i-Cp)(Flu)$ZrCl_2$ (**2**) and *i*-Pr(3-Me-Cp)(Flu)$ZrCl_2$ (**3**) and methylaluminoxane.[15] In particular, by using an analytical procedure which fully exploits the information contained in the spectra, we could determine the microstructure of the E−N copolymers synthesized with **2** and **3** at the pentad level.[16] This has allowed for more accurate tests on the statistical model best describing E−N copolymerization with C_1-symmetric catalysts[17−20] and for the study of the influence of ligand substitution of these catalysts on the polymerization mechanism.[21,22] It was found that norbornene and ethylene are inserted at the same site by a Cossee's migratory mechanism and a subsequent backskip of the copolymer chain to its original position after every insertion (Figure 4). In that work we found quite instructive the comparison with the spectra of E−N copolymers produced by C_s-symmetric Me_2C(Flu)(Cp)$ZrCl_2$ (**1**)-based catalyst, which is known to be highly selective in producing E−N copolymers with *racemic* ENNE diads.[23] The need for a deeper and more quantitative investigation of the spectra of these copolymers, which are more difficult to be interpreted than those of E−N copolymers with *meso* ENNE diads, motivates the present work.

Here we shall present the microstructural analysis by ^{13}C NMR of copolymers obtained with metallocene **1**. Our results on copolymer microstructures obtained at the tetrad level will be discussed and used to evaluate

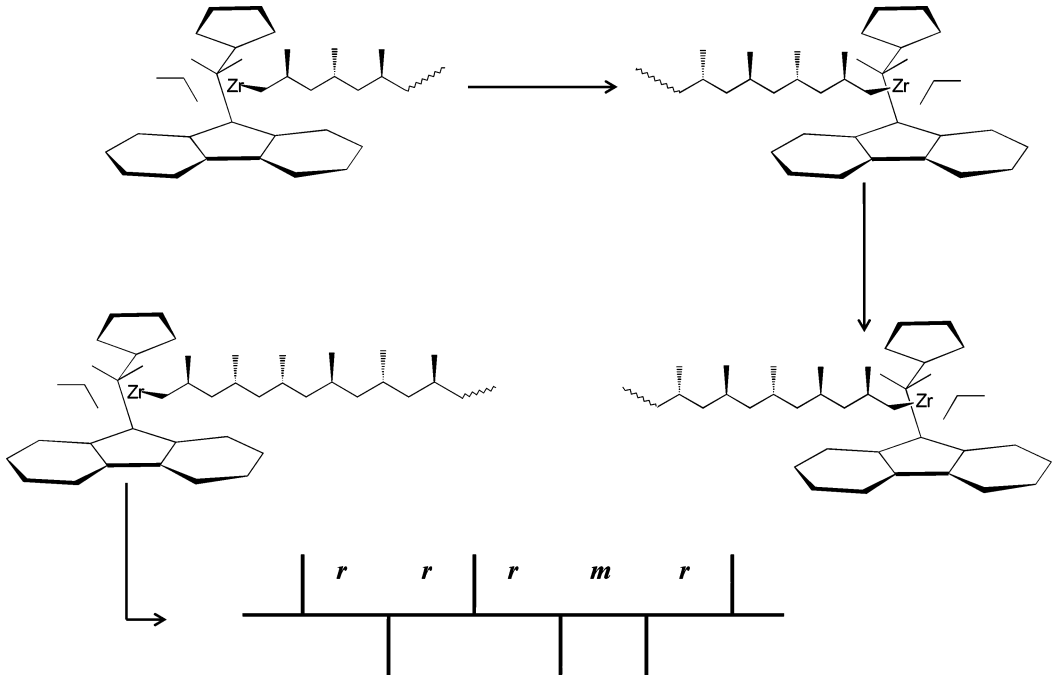

Figure 3. Errors by site epimerization in syndiotactic polypropylene by site control with C_s-symmetric metallocenes.

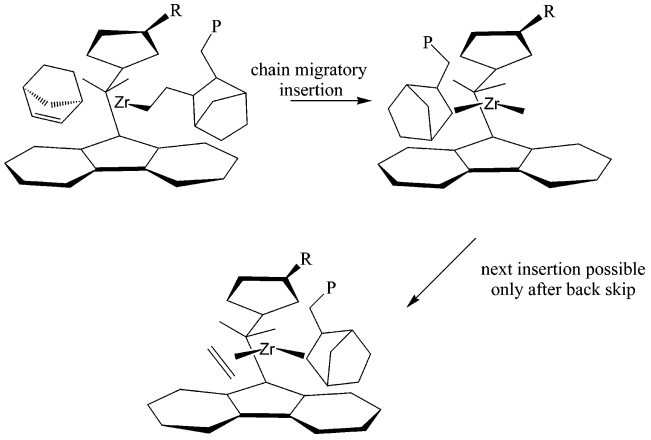

Figure 4. Mechanisms for alternating isotactic E−N copolymerization with C_1-metallocenes.[15]

and test the copolymerization statistical models. Finally, we will present insights into olefin polymerization mechanisms operating in these systems, obtained from such an analysis.

Results

Copolymer Synthesis. Ethylene−norbornene copolymerizations with the C_s-symmetric *i*-Pr [(Cp)(9-Flu)]-$ZrCl_2$ (**1**) metallocene (Chart 1) were investigated to obtain evidence on proposed olefin polymerization mechanisms. Ethylene−norbornene copolymerizations were carried out at 30 °C at atmospheric ethylene pressure in the presence of methylaluminoxane at [Al]/[Zr] molar ratio of 3000. A wide range of [N]/[E] feed ratios was investigated. The polymerization tests were designed to study copolymer microstructures, that is, low comonomer conversion and low polymer concentration in the polymerization medium. Norbornene conversion was kept below 10%. The norbornene content in the copolymer was obtained by ^{13}C NMR spectroscopy. Molecular weights were estimated by SEC measurements. The results concerning the synthesis and the characterization of selected copolymers are summarized in Table 1. Polymer yields of copolymerization with **1** are higher than those with C_2-symmetric *ansa* metallocenes such *rac*-$Et(Ind)_2ZrCl_2$ (Ind = indenyl) under the same conditions.[9] In general, C_s-symmetric $R_2C[(Cp)(9\text{-}Flu)]ZrCl_2$ showed higher activity than the C_2-symmetric metallocenes.[5] As in almost all E−N copolymerizations by *ansa*-metallocenes, the increase in N concentration in a polymerization feed results in a decrease in catalytic activity, likely due to the facility of N coordination to the active sites, and in an increase of N content in the copolymer up to a plateau. Polydispersity is consistent with single site catalysis. To keep low the comonomer conversion, the polymerization time varies from one copolymerization run to the other; this may have an influence on the molecular weight. Thus, it is difficult to comment on the different values observed in the series.

Table 1. Ethylene−Norbornene Copolymerizations with the Catalysts *i*-Pr(Cp)(Flu)$ZrCl_2$ (1): mol % of Norbornene in the Copolymer, Productivity, and Molecular Weight[a]

entry	feed ratio [N]/[E]	N (mol %)[b]	activity[c]	M_n[d] × 10^3	M_w/M_n[d]
1	0.11		2341	37.20	2.0
2	0.25		1669	44.23	1.8
3	0.43	24.40	930	51.37	2.4
4	0.67	28.19	866	48.75	1.9
5	1.00	30.40	540	46.05	1.6
6	2.33	40.18	247	50.30	1.5
7	4.00	47.12	151	59.76	2.3
8	9.00		90	42.66	1.6

[a] Toluene as a solvent, MAO as a cocatalyst, 30 °C, $P_E = 1.01$ atm. [b] Mol % of norbornene calculated by analysis of ^{13}C NMR spectra (see text). [c] Activity = kg of polymer/(mol Zr h). [d] Measured by SEC at 145 °C in 1,2-dichlorobenzene.

^{13}C NMR Analysis. A detailed analysis of the copolymer ^{13}C NMR spectra and their correct assignment are crucial for obtaining a description of the copolymer microstructure suitable to gain deeper insight into the polymerization mechanism. A typical chain representing E−N copolymers produced by **1**, along with the adopted carbon numbering and denomination, is sketched in Figure 5. This chain contains norbornene in alternating

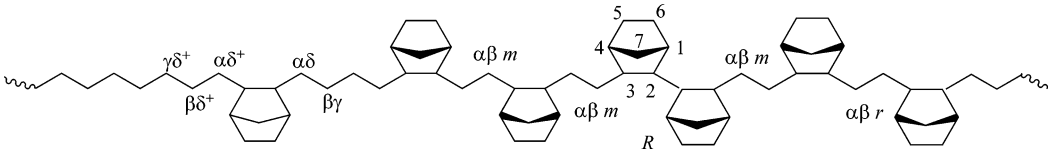

Figure 5. Copolymer chain and nomenclature.

Table 2. Assignments of ^{13}C NMR Chemical Shifts for Carbons of Norbornene and Ethylene Units in E−N Copolymers

carbon[a]	chemical shift (ppm)	sequences
	Ethylene[b,c]	
$S_{\delta+\delta+}$	27.74	EEE*E*EEE
$S_{\delta\delta+}$	27.80	ENE*E*EE
$S_{\beta\delta+}$	27.93	EN*E*EE
$S_{\alpha\beta}$ *r*	28.04	EN*E*NE
$S_{\gamma\delta+}$	28.05	ENE*E*E
$S_{\alpha\delta+}$	28.13	EN*E*EE
$S_{\alpha\delta}$, $S_{\gamma\delta}$	28.18	EN*E*EN, NE*E*EN
$S_{\beta\gamma}$	28.39	EN*E*EN
$S_{\alpha\beta}$ *m*	28.56	EEN*E*NEE
$S_{\alpha\beta}$ *m*	28.61	NEN*E*NEE
$S_{\alpha\beta}$ *m*	28.66	NEN*E*NEE
$S_{\alpha\beta}$ *m*	28.70	NEN*E*NEN
	Norbornene[c]	
C5/C6	28.33	E*N*E
C7	30.89	EE*N*EE
C7 *m*	30.96	NE*N*EE
C7 *r*	30.98	NE*N*EN
C7 *m*	31.04	NE*N*EN
C1/C4 *r*	39.54	NE*N*EN
C4 *m*	39.54	1/2 NE*N*EE
C1/C4	39.57	EE*N*EE
C1 *m*	39.86	1/2 NE*N*EE
C1/C4 *m*	40.00	NE*N*EN
C3 *m*	45.09	1/2 NE*N*EE
C2/C3 *r*	45.21	NE*N*EN
C2 *m*	45.78	1/2 NE*N*EE,
C2/C3 *m*		NE*N*EN

[a] The ^{13}C NMR spectra were measured in $C_2D_2Cl_2$ at 105 °C; chemical shifts are referred to HDMS. [b] The Greek subscripts indicate the distance of the observed secondary carbon atom S from the closest norbornene carbons. [c] See Figure 5 for carbon numbering and denomination.

sequences, both *meso* and *racemic*, norbornene isolated between ethylene blocks, and *racemic* NN diads.

The progress in assignments of the spectra of E−N copolymers has been recently reviewed.[7] An updated set of assignments of the ^{13}C NMR spectra, achieved with the contributions by various authors, for the carbons of alternating and isolated units observable in the spectra of E−N copolymers prepared with catalyst **1** is collected in Table 2. Signals involved in sequences with *racemic* norbornene diblocks are summarized in Table 3.

The spectra of two samples of E−N copolymers prepared with **1** and having different norbornene content are compared in Figures 6 and 7. Entry 3 has 24.4 mol % of norbornene, while entry 7 has 40.2 mol %.

The spectrum at low norbornene content is relatively simple (Figure 6). The signals in the range 28.58−28.72 ppm due to $S_{\alpha\beta}$ of *meso* alternating ENENE and at 45.77 ppm due to C2/C3 of meso alternating NENEN are clearly visible; the expansion of the region between 44.8 and 46.0 ppm shows also indications of C2/C3 signals at 45.21 ppm diagnostic of *racemic* alternating sequences. The latter are present in the spectra of all samples. The detailed analysis of these spectra allows us to quantify the alternating *meso* and *racemic* sequences. As we shall see later, this provides new insights into polymerization mechanisms.

Table 3. Assignments of ^{13}C NMR Chemical Shifts for Carbons of Norbornene and Ethylene Units Affected by NN Diads in the E−N Copolymers Studied in This Work

carbon	chemical shift (ppm)	sequences[a]
	Ethylene	
$S_{\alpha\beta}$ *m*	29.11	N*E*NN (*R*)
	Norbornene	
C5 *R*	27.58	ENNE
C6 *R*	29.37	ENNE
C7 *R*	31.57	ENNE
C1 *R*	38.93	ENNE
C4 *R*	39.80	ENNE
C2 *R*	45.62	ENNE
C3 *R*	48.07	ENNE

[a] See Figure 5 for the denomination of meso (*m*) alternating NEN sequence and NENN (*R*) sequence.

The spectrum at high norbornene content in Figure 7 clearly shows that the **1** precatalyst, in combination with MAO under the polymerization conditions used, produces only racemic NN sequences. Indeed, the signals at 26.24 and 29.68 ppm (C5 and C6) and at 45.96, 46.05, 46.50, and 47.12 ppm diagnostic of *meso* ENNE sequences are absent.[11,12] No norbornene triads are observed. The complexity of these spectra here appears to arise from the presence of possible different stereoisomers of NENENNENENE sequences: the central *racemic* ENNE sequence can be surrounded by *rac*−*rac, meso*−*meso*, or *rac*−*meso* NENEN sequences.

Tetrad Microstructure and Polymerization Statistics of E−N Copolymers Obtained by *i*-Pr [(Cp)-(9-Flu)]ZrCl$_2$. The spectra of these copolymers are not so neat as those of copolymers which contain only *meso* NN blocks or no NN blocks at all, for which we were able to gather information on the polymer microstructure at pentad level with some information even on heptad sequences.[15] Nevertheless, it has been possible to use our standard analytical procedure,[11−13] which uses the information from the whole spectrum, to derive the microstructure of the series of copolymers reported in Table 1 in order to get an estimate of the copolymerization parameters as accurate as possible. The procedure adopted along with the definition of the variables involved has been recently described in great detail.[12] In Table 4 we represent the results of the analysis of six samples (entries 3−7) through the molar fractions of tetrads, even though some higher level splittings have been accounted for in the calculations.

Although the complexity of these spectra does not allow for a complete pentad resolution, the analysis is sufficient to test both the first-order and the second-order statistics.[24,25] Indeed, in the past few years, we have used tetrad information on E−N copolymers obtained with catalysts *rac*-Et(Ind)$_2$ZrCl$_2$ (**4**), *rac*-Me$_2$Si(Ind)$_2$ZrCl$_2$ (**5**), and Me$_2$Si(Me$_4$Cp)(N^{t}Bu)TiCl$_2$ (**6**) to determine the copolymerization parameters and clarify possible statistical models of copolymerization, discriminating between ultimate and penultimate effects.[13] In those cases the second-order Markov model (M2) showed better fits than the first-order Markov model (M1).

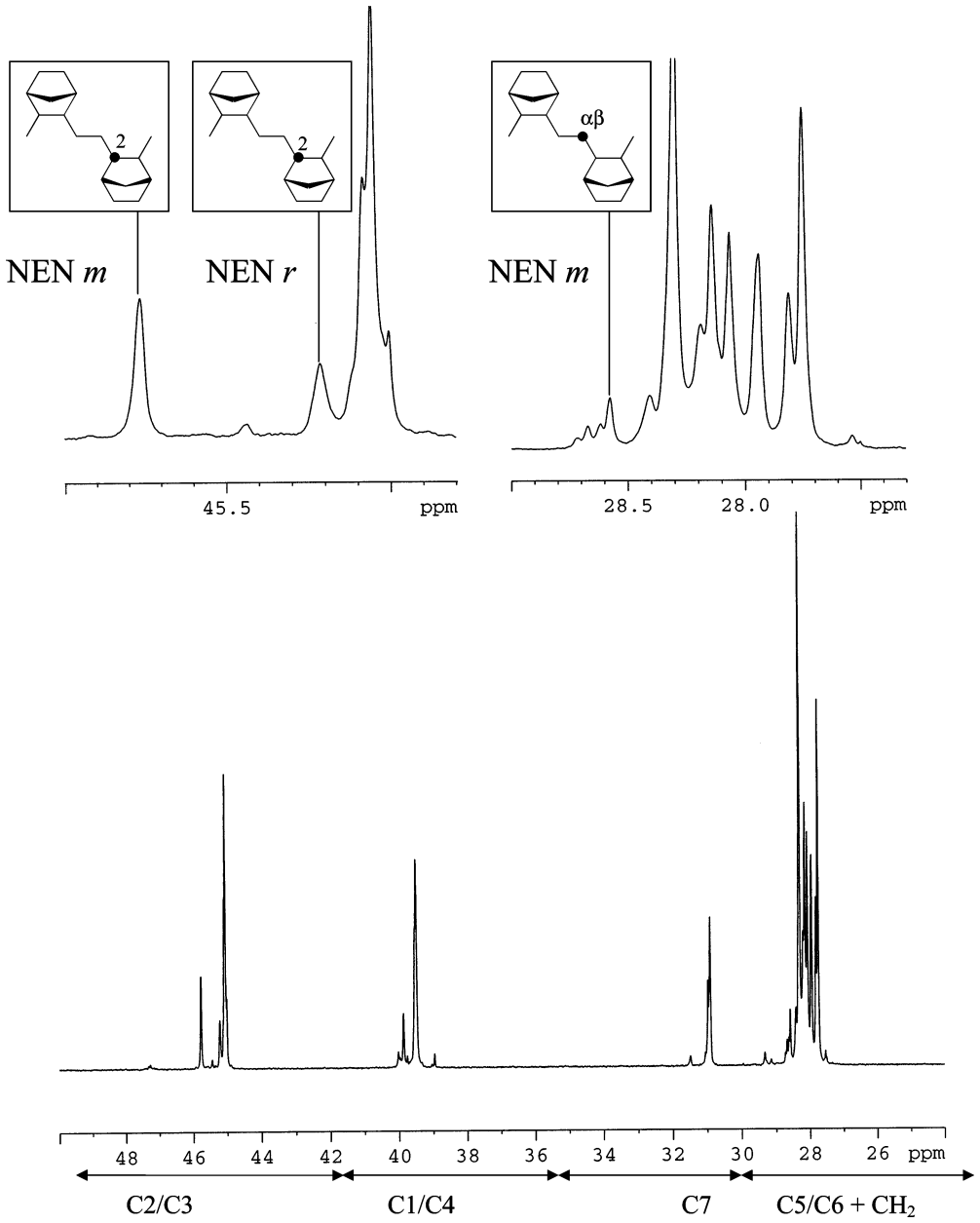

Figure 6. Spectrum of an E−N copolymer sample, prepared with metallocene **1**, entry 3, with N content of 24.4 mol %.

Table 4. Tetrad Least-Squares Fitting for E−N Copolymer Samples Obtained with Catalyst *i*-Pr(Cp)(Flu)ZrCl$_2$ (1)

entry	feed ratio [N]/[E]	EEEE	NEEE	NEEN	ENEE	NNEE	NENE	NNEN	ENNE	R^2
3	0.43	0.2338	0.2268	0.0551	0.3316	0.0053	0.1413	0.0023	0.0038	0.9996
4	0.67	0.1512	0.2197	0.0733	0.3555	0.0108	0.1760	0.0054	0.0081	0.9992
5	1.00	0.1525	0.1490	0.1029	0.3399	0.0150	0.2187	0.0096	0.0123	0.9972
6	2.33	0.0645	0.0623	0.1003	0.2412	0.0218	0.4395	0.0397	0.0307	0.9971
7	4.00	0.0524	0.0134	0.0704	0.1233	0.0309	0.5043	0.1265	0.0787	0.9977

The results obtained here from the tetrad description of the microstructure of the copolymers prepared with **1** are presented in Table 5. Only for the samples at low N content the M2 statistics gives very good fitting estimated standard error (ese) superior to M1. In all the other cases the agreement is not good with both models. These results maybe related to low quality of the fitting of NMR data due to the low resolution of the spectra. At any rate the reactivity ratios (r_1 and r_2 and r_{11}, r_{21}, and r_{12}) show rather coherent values in the whole series: the values of r_{11} are very close to r_1 and r_{12} values are close to r_2; moreover, these parameters are remarkably independent of the feed ratio. The average r_1 values above 1 and the low r_2 value of 0.04 indicate a preference for insertion of ethylene over norbornene into an active Mt−E* center and clearly illustrate that catalyst **1** has a tendency to produce alternating microstructures at high N/E feed ratios. However, the ^{13}C NMR spectrum in Figure 7 clearly reveals that this catalyst is able to produce copolymers with *rac*-ENNE sequences. Worth noting is that the average r_2 and r_1 values are very close to those calculated by means of the Finemann and Ross equations by Kaminsky.[26] This picture confirms that with this fluorenyl *ansa*-metallocene the insertion of a monomer unit is little affected by the penultimate monomer unit, in agreement with

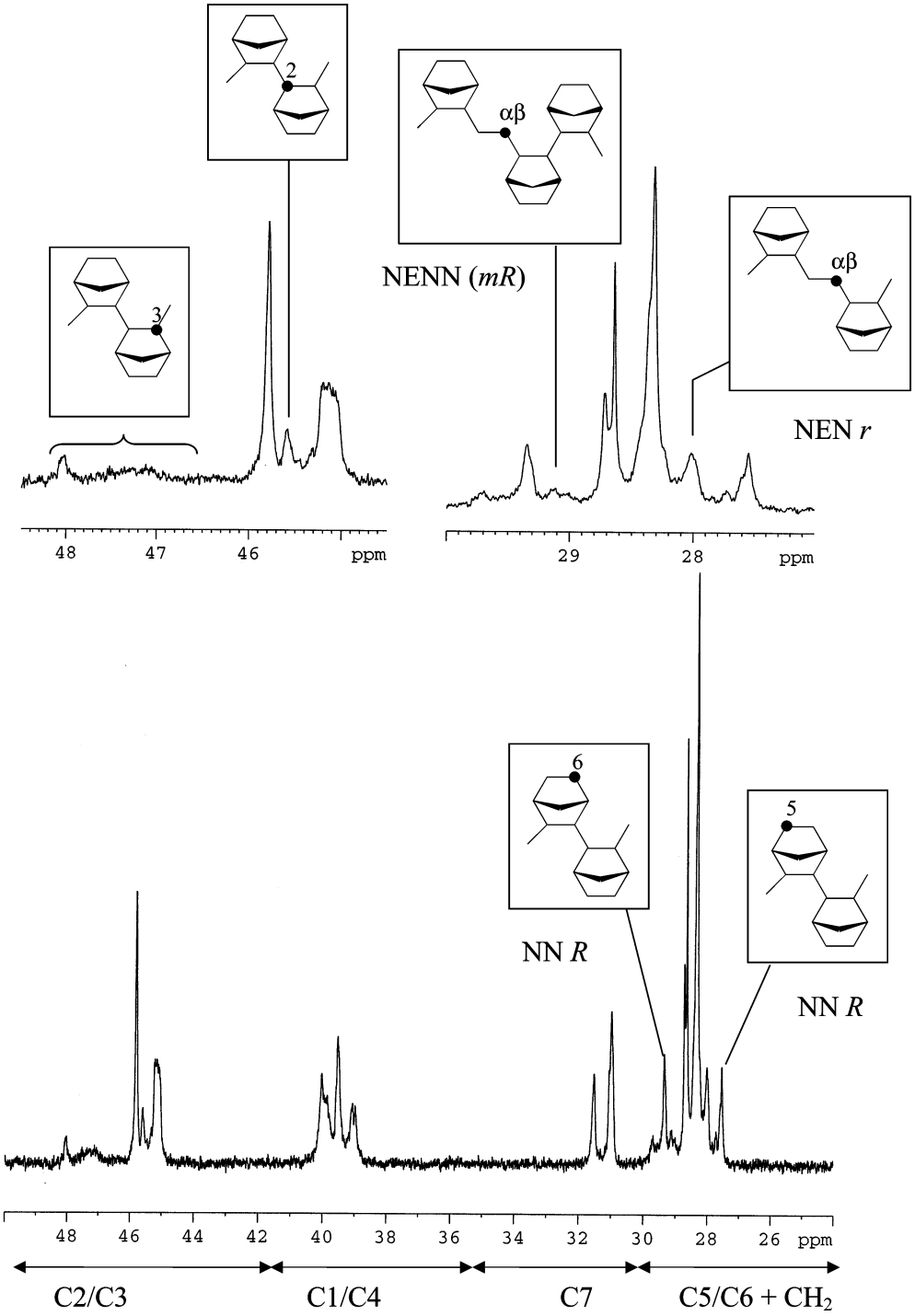

Figure 7. Spectrum of an E−N copolymer sample, prepared with metallocene **1**, entry 7, with N content of 40.5 mol %.

Table 5. Reactivity Ratios of E−N Copolymerizations with Catalyst *i*-Pr(Cp)(Flu)ZrCl$_2$ (1) Calculated Using First- and Second-Order Markovian Models from Tetrad Distribution

			M1			M2			
entry	feed ratio N/E	N (mol %)	r_1	r_2	(ese)	r_{11}	r_{21}	r_{12}	(ese)
3	0.43	24.40	0.92	0.03	0.0046	0.89	1.01	0.04	0.000 02
4	0.67	28.19	1.10	0.03	0.0138	0.95	1.36	0.05	0.0017
5	1.00	24.68	1.41	0.04	0.0200	1.30	1.50	0.05	0.0193
6	2.33	40.18	1.27	0.04	0.0168	1.13	1.30	0.04	0.0166
7	4.00	47.12	1.02	0.06	0.0201	0.84	1.05	0.07	0.0171

a previous observation by Kaminsky, who found that E−N copolymerization with **1** follows first-order Markov statistics.[27]

These features are evident in Figure 8A,B, where the NMR-measured tetrad distributions obtained by the methodology used in this work are compared with those calculated according to first- and second-order Markovian models. The two representative copolymer samples selected are those whose spectra are displayed in Figures 6 and 7. The first sample with low N content

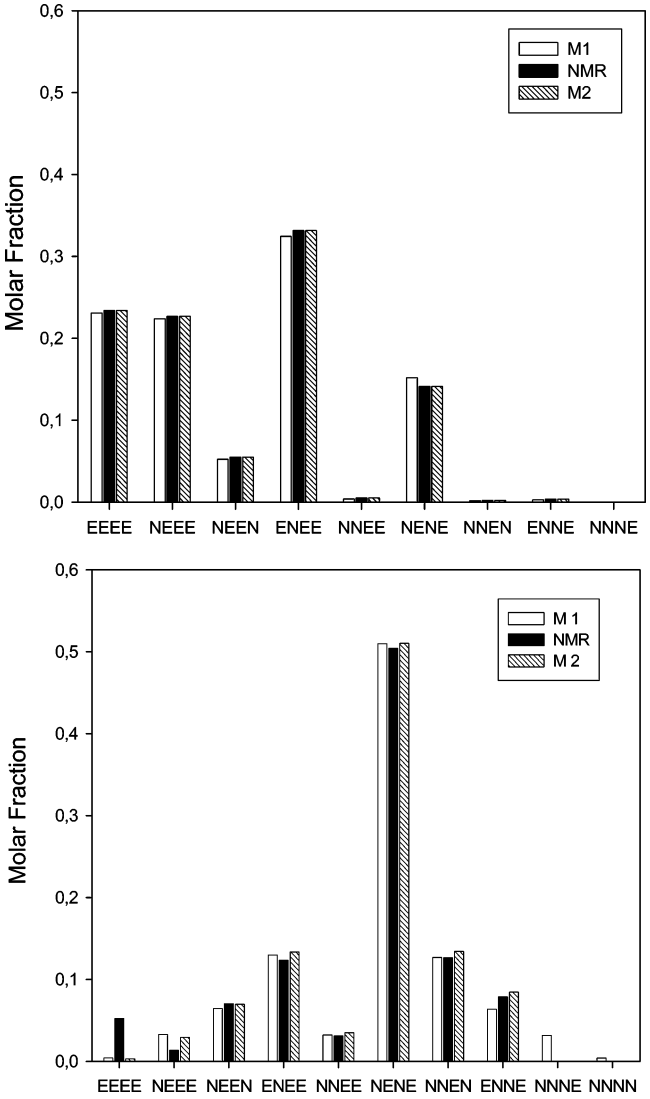

Figure 8. Experimental and calculated tetrad distribution for E−N copolymer samples prepared with *i*-Pr(Cp)(Flu)$ZrCl_2$ (**1**) at feed ratio 0.43 (entry 3) (A) and at feed ratio 4.00 (entry 7) (B). Black: experimental data obtained from NMR; white: according to model M1; dashed: according to model M2.

(Figure 8A) shows a very good agreement with all tetrad molar fractions. The highly alternating (NENE 50%) sample 7 presents a large discrepancy at EEEE and NEEE tetrads, suggesting the possible inhomogeneity of this copolymer.[28] In this sample we also note a significant amount of NN diads, while we do not observe NNN triads to be expected according to M1. The absence of NNN blocks indicates a certain influence of the penultimate inserted norbornene units. Thus, it is confirmed that steric interactions are important in determining the polymerization statistiscs. In E−N copolymerizations with fluorenylmetallocenes *i*-Pr(3-R′-Cp)(Flu)$ZrCl_2$ **1** and **2** (R′ = H and Me, respectively), only the ultimate monomer inserted unit influences the next insertion (M1), with metallocene **3** (R′ = *i*-Pr) next insertion is influenced by the penultimate unit (M2) due to the steric interactions between *i*-Pr and copolymer chain.

Mechanistic Considerations. The observation of only *racemic* ENNE sequences in E−N copolymers prepared by C_s-symmetric catalyst **1** is convincing evidence that a Cossee-type mechanism holds also for E−N copolymerizations (Figure 9). The olefin insertion involves the migration of the polymer chain to the site occupied by the coordinated monomer. Indeed, when a norbornene is inserted at one of the two enantiotopic sites formed after the activation of the prochiral metallocene **1**, the polymer chain migrates to the site of the monomer approach. Thus, the next norbornene is inserted at the opposite enantiotopic site with the opposite face.

Following Cossee's migratory insertion mechanism, we would expect the formation of only *meso* NEN alternating sequences in these copolymers (Figure 10). Quite instructive is the presence of *meso* and *racemic* NEN sequences observable in the spectra in Figures 5 and 6 and in the spectra of all the copolymers of this series. Their molar fractions calculated through our procedure are plotted in Figure 10 against the N content in copolymer or the N concentration in the feed.

In principle, the formation of NEN *racemic* sequences could derive either from an error in stereocontrol or from chain backskip as the formation of *rrrrmrrrr* sequences in syndiotactic polypropylene (Figure 11). The high stereocontrol[11] in ENNE sequences obtained by **1** along with high stereoregularity in N−E−N sequences in copolymers obtained by C_2-symmetric metallocenes supports the conclusion that NEN racemic sequences here should derive from occasional backskip (chain migration without insertion). The amount of *racemic* NEN sequences indicates that probability of chain backskip is relatively high with respect to that observed in syndiotactic propylene polymerization[4] mediated by the same catalyst under the same polymerization conditions. This effect seems to be due to norbornene strong coordinating ability which could influence the competition between site epimerization and chain propagation. By using coordinatively diverse counterions, Marks[4] has shown that it is possible to modulate site epimerization and propagation rates and thus the propylene syndiotacticity of this catalyst. It was also well-known that **1** syndiotacticity decreases in polar solvents such as CH_2Cl_2 and 1,3-dichlorobenzene.[29] The DFT calculations of relative formation energies performed by Yoshida et al.[30] indicated that the N coordination to a Ti−E* species in the bis(pyrrolidimine)Ti complex/MAO system results to be more stable than the corresponding E-coordinated species by 8.33 kJ/mol. This is indicative of dominant N coordination to the Ti center of the E-last-inserted species. The coordination of highly nucleophilic and

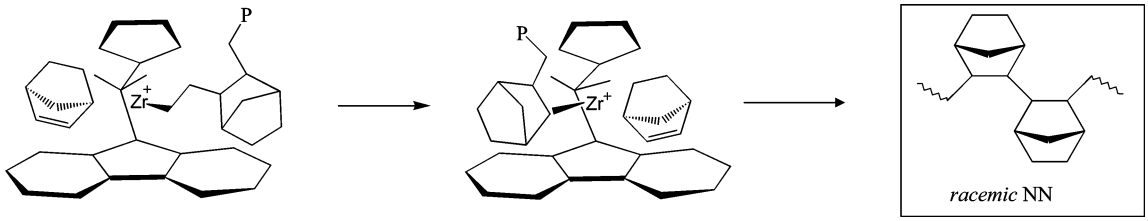

Figure 9. Cossee-type mechanism for E−N copolymerizations with with C_s-symmetric metallocene **1**.

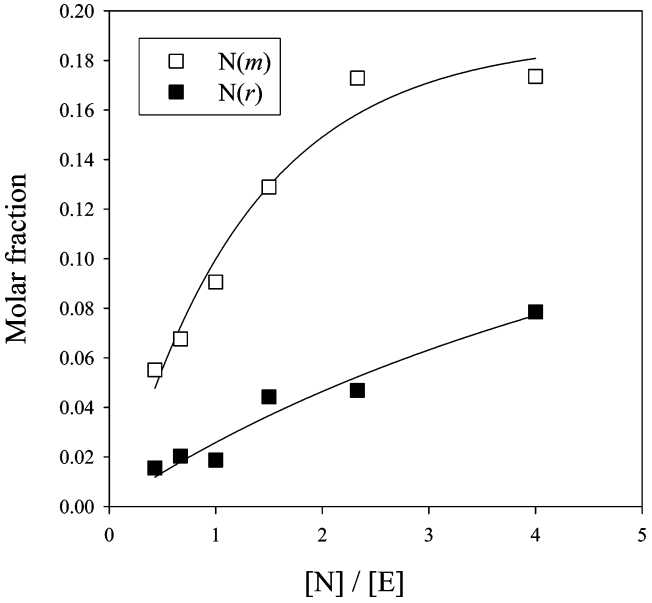

Figure 10. *Meso* and *racemic* NEN molar fractions calculated through our procedure[15] against the [N]/[E] feed ratio.

sterically encumbered N to the E-last-inserted active species would reduce the electrophilicity of the active species. Thus, here norbornene coordination slows down the propagation rate and favors the polymer chain to move away leading to *racemic* NEN sequences.

Conclusions

A series of E−N copolymers have been synthesized with C_s-symmetric metallocene **1**. The microstructural analysis by ^{13}C NMR of copolymers obtained has been completely obtained at tetrad level thanks to the use of our methodology which exploits all the peak areas of the spectra and accounts for the stoichoimetric requirements of the copolymer chain. Copolymers with 40.2 mol % of norbornene are highly alternating (NENE 50 mol %) and contain a significant amount of ENNE (8 mol %) and no ENNN sequences. Accurate test of the M1 and M2 statistical models allowed us to conclude that norbornene and ethylene copolymerizations mediated by **1** follow M1 statistics. The values of r_{11} are very close to r_1, and r_{12} values are close to r_2. The average r_1 values above 1 and the low r_2 value of 0.04 indicate the tendency of catalyst **1** to produce alternating microstructures at high N/E feed ratios.

Comparisons with results obtained with **2** and **3**[15] confirmed that steric interactions are important in determining the polymerization statistiscs. With metallocenes **1** and **2** (R′ = H and Me, respectively) only the ultimate monomer inserted unit influences the next insertion (M1), with metallocene **3** (R′ = *i*-Pr) next insertion is influenced by penultimate unit (M2) due to the steric interactions between *i*-Pr and copolymer chain. Finally, we have found that the two monomers are inserted according to a Cossee's migratory mechanism and that backskips of the copolymer chain to its

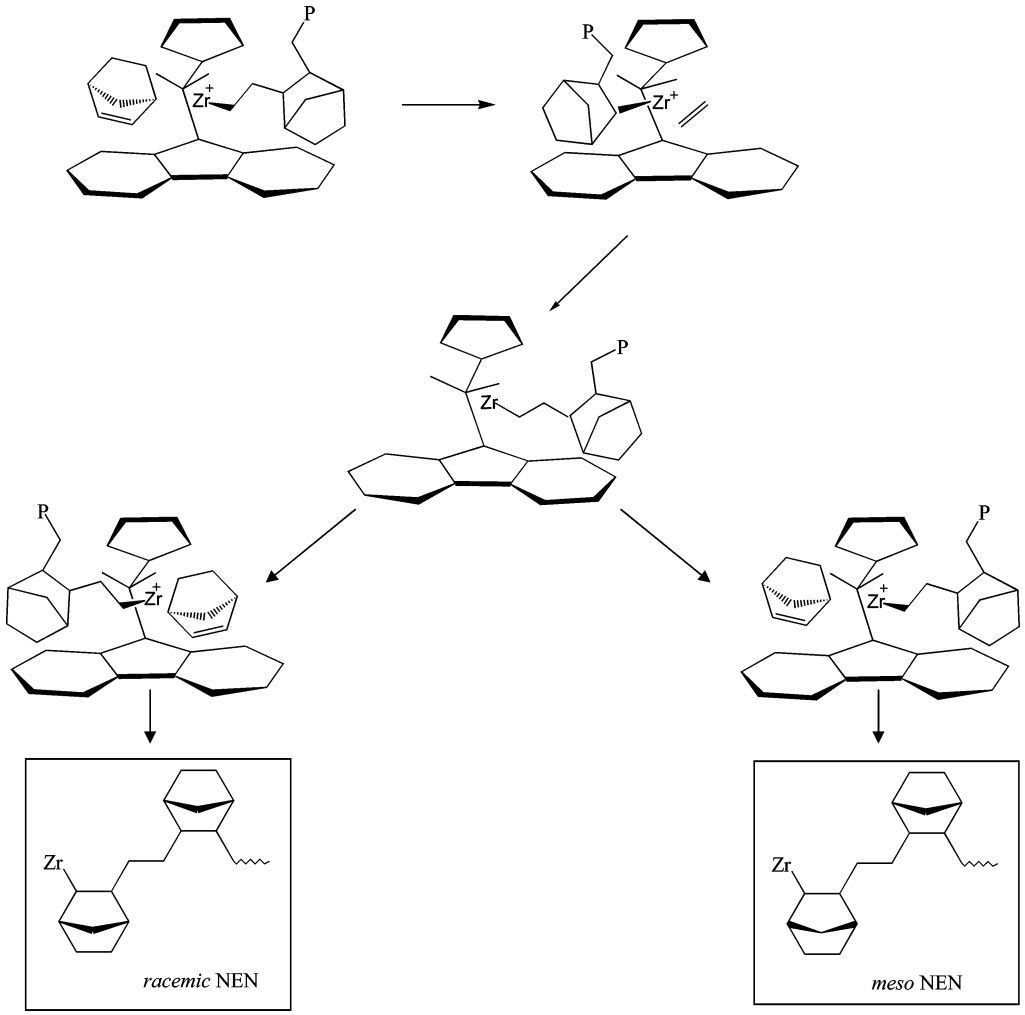

Figure 11. Origin of *meso* and *racemic* NEN sequences in E−N copolymerization with C_s-metallocene.

original position occur, causing the formation of both *meso* and *racemic* NEN sequences. The probability of chain backskip is relatively high with respect to that observed in syndiotactic propylene polymerization under the same polymerization conditions. This effect seems to be due to norbornene strong coordinating ability which could influence the competition between site epimerization and chain propagation.

Experimental Part

General Conditions. All experiments were performed under dry nitrogen in a drybox or using standard Schlenk line techniques. Methylaluminoxane (MAO) (10 wt % as toluene solution, Crompton) was dried (50 °C, 3 h, 0.1 mmHg) before use. Toluene was dried and distilled from sodium under a nitrogen atmosphere. *i*-Pr(Cp)(Flu)$ZrCl_2$ was purchased from Boulder. Nitrogen and ethylene gases were dried and deoxygenated by passage over columns of $CaCl_2$, molecular sieves, and BTS catalysts. Norbornene was distilled from sodium and used as stock solution in toluene.

Polymer Synthesis. A typical ethylene−norbornene copolymerization experiment with metallocene **1** was carried out in a 250 mL round-bottomed Schlenk flask in an oil bath thermostated at 30 °C. After three vacuum−nitrogen cycles, norbornene was introduced in the reactor. Toluene (100 mL) was then cannula transferred, and MAO was added as a toluene solution ([Al] = 3 mol L^{-1}). After evacuation of the nitrogen, the solution was saturated with ethylene at atmospheric pressure. The reacting medium was stirred for 30 min (stirring rate of 1000 rpm) in order to dissolve the ethylene and to homogenize the medium. The catalyst was then added as a toluene solution freshly prepared (typically [Zr] = 0.010 mmol L^{-1}, Al/Zr = 3000). The pressure of ethylene, temperature, and stirring rate were kept constant during the polymerization. Copolymerization reactions were stopped before the medium would become heterogeneous and before 10% of the initially introduced norbornene was consumed. After the given reaction time, the polymerization reactions were quenched by slow addition of ethanol initially, and then mixture was poured into acidic ethanol. The precipitated polymer was washed with EtOH and dried under vacuum.

Ethylene concentration in toluene was calculated according to Henry's law, as already described.[11] Ethylene was used instead of nitrogen to purge the Schlenk flask before introducing the reagents.

Size Exclusion Chromatography The molar mass distribution (MMD) and polydispersity were performed on a high-temperature dual-detector size exclusion chromatography (SEC) system. The SEC system was a GPCV2000 from Waters (Milford, MA) that uses two on-line detectors: a differential viscometer (DV) and a differential refractometer (DRI) as concentration detector. The description of this SEC-DV system has been reported elsewhere.[31] The experimental conditions were *o*-dichlorobenzene + 0.05% 2,6-di-*tert*-butyl-4-methylphenol (BHT, antioxidant) as mobile phase, 0.8 mL/min as flow rate, and a column temperature of 145 °C. The column set was composed of three GMH_{XL}-HT columns from TosoHaas (Stuttgart, Germany). The universal calibration was constructed from 18 narrow MMD polystyrene standards, with the molar mass ranging from 162 to 5.48×10^6 g/mol.

^{13}C NMR Characterization. The copolymers were dissolved in $C_2D_2Cl_4$. HMDS was used as internal reference. Analyses were performed at 103 °C on a Bruker AV-400 spectrometer in the PFT mode. Composite pulse decoupling was used to remove $^{13}C-{}^{1}H$ couplings.

The norbornene content of the copolymers was calculated according to the formula $[2I(C_7) + I(C_1-C_2) + I(C_2-C_3)] \times 100/3I(CH_2)$, where $I(CH_2)$, $I(C_7)$, $I(C_1-C_2)$, and $I(C_2-C_3)$ are the peak areas in the ranges 26−30, 30−36, 34−42, and 43−54 ppm of ^{13}C NMR spectra as previously reported.[11]

Calculation of Tetrad Distribution and Reactivity Ratios. The tetrad distributions were calculated from the segment molar fractions: $f(m)$, f_0, f_1, f(isl), f_E(isl), as defined in ref 11, and f_N(isot), which represents pentad NENEN. The the copolymerization parameters were determined as described in ref 13.

Acknowledgment. We thank Mr. G. Zannoni for his valuable cooperation in NMR analysis.

References and Notes

(1) (a) Brintzinger, H. H.; Fischer, D.; Mülhaupt, R.; Rieger, B.; Waymouth, R. *Angew. Chem., Int. Ed. Engl.* **1995**, *34*, 1143. (b) Resconi, L.; Cavallo, L.; Fait, A.; Piemontesi, F. *Chem. Rev.* **2000**, *100*, 1253−1345.

(2) (a) Ewen, J. A.; Jones, R. L.; Razavi, A.; Ferrara, J. D. *J. Am. Chem. Soc.* **1988**, *110*, 6255−6256. (b) Spaleck, W.; Antberg, M.; Dolle, V.; Klein, R.; Rohrmann, J.; Winter, A. *New J. Chem.* **1990**, *14*, 499. (c) Ewen, J. A.; Elder, M. J.; Jones, R. L.; Haspeslagh, L.; Atwood, J.; Bott, S. G.; Robinson, K. *Makromol. Chem., Rapid Commun.* **1991**, *48/49*, 253. (d) Razavi, A.; Atwood, J. L. *J. Organomet. Chem.* **1995**, *497*, 105.

(3) (a) Cossee, P. *Tetrahedron Lett.* **1960**, 12. (b) Cossee, P. *Tetrahedron Lett.* **1960**, 17.

(4) (a) Ewen, J. A.; Elder, M. J.; Jones, R. L.; Curtis, S.; Cheng, H. N. In *Catalytic Olefin Polimerization; Stud. Surf. Sci. Catal.*; Keii, T., Soga, K., Eds.; Elsewier: New York, 1990; p 439. (b) Farina, M.; Terragni, A. *Makromol. Chem., Rapid. Commun.* **1993**, *14*, 791. (c) Razavi, A.; Peters, L.; Nafpliotis, L.; Vereecke, D.; Den Dauw, K. *Macromol. Symp.* **1995**, *89*, 345. (d) Busico, V.; Cipullo, R.; Talarico, G.; Segre, A. L.; Caporaso, L. *Macromolecules* **1998**, *31*, 8720−8724. (e) Veghini, D.; Henling, L. M.; Burkhardt, T. J.; Bercaw, J. E. *J. Am. Chem. Soc.* **1999**, *121*, 564−573. (f) Marks, T. J.; Chen, M. C.; Roberts, J. A. S. *J. Am. Chem. Soc.* **2004**, *126*, 4605−4625.

(5) (a) Kaminsky, W.; Noll, A. *Polym. Bull. (Berlin)* **1993**, *31*, 175. (b) Kaminsky, W. *Macromol. Chem. Phys.* **1996**, *197*, 3907−3945. (c) Kaminsky, W.; Bark, A.; Steiger, R. *J. Mol. Catal.* **1992**, *72,* 109−119. (d) Kaminsky, W.; Bark, A.; Arndt, M. *Makromol. Chem., Macromol. Symp.* **1991**, *47*, 83−93. Arndt, M.; Kaminsky, W. *Macromol. Symp.* **1995**, *97*, 225−46. (c) Arndt, M.; Engehausen, R.; Kaminsky, W.; Zoumis, K. *J. Mol. Catal A: Chem.* **1995**, *101*, 171−178.

(6) Ruchatz, D.; Fink, G. *Macromolecules* **1998**, *31*, 4674−80.

(7) Tritto, I.; Boggioni, L.; Ferro, D. R. *Coord. Chem. Rev.*, in press.

(8) Tritto, I.; Boggioni, L.; Sacchi, M. C.; Locatelli, P.; Ferro, D. R.; Provasoli, A. *Macromol. Rapid Commun.* **1999**, *20*, 279.

(9) Tritto, I.; Boggioni, L.; Sacchi, M. C.; Locatelli, P.; Ferro, D. R.; Provasoli, A. In *Metalorganic Catalysts for Synthesis and Polymerization*; Kaminsky, W., Ed.; Springer: Berlin, 1999; p 493.

(10) Provasoli, A.; Ferro, D. R.; Boggioni, L.; Tritto, I. *Macromolecules* **1999**, *32,* 6697−6706.

(11) Tritto, I.; Marestin, C.; Boggioni, L.; Zetta, L.; Provasoli, A.; Ferro, D. R. *Macromolecules* **2000**, *33*, 8931.

(12) Tritto, I.; Marestin, C.; Boggioni, L.; Sacchi, M. C.; Brintzinger, H. H.; Ferro, D. R. *Macromolecules* **2001**, *34*, 5770−5777.

(13) Tritto, I.; Boggioni, L.; Jansen, J. C.; Thorshaug, K.; Sacchi, M. C.; Ferro, D. R. *Macromolecules* **2002**, *35*, 616.

(14) Thorshaug, K.; Mendichi, R.; Tritto, I.; Trinkle, S.; Friedrich, C.; Mülhaupt, R. *Macromolecules* **2002**, *35*, 2903.

(15) Tritto, I.; Boggioni, L.; Ferro, D. R. *Macromolecules* **2004**, *37*, 9681−9693.

(16) For details on the methodology to perform microstructural analysis by ^{13}C NMR of E−N copolymers, see refs 11 and 13. For general reviews on ^{13}C NMR in (a) ethylene based copolymers, see: Randall, J. C. *J. Macromol. Sci., Rev. Macromol. Chem. Phys.* **1989**, *C29.* 201. (b) Polypropylene: Busico, V.; Cipullo, R. *Prog. Polym. Sci.* **2001**, *26*, 443 and references therein.

(17) Arndt, M.; Beulich, I. *Macromol. Chem. Phys.* **1998**, *199*, 1221.

(18) Herfert, N.; Montag, P.; Fink, G. *Makromol. Chem.* **2001**, *94*, 3167.

(19) Wendt, R. A.; Mynott, R.; Fink, G. *Macromol. Chem. Phys.* **2002**, *203*, 2531.

(20) Arndt, M.; Kaminsky, W.; Schauwienold, A.-M.; Weingarten, U. *Macromol. Chem. Phys.* **1998**, *199*, 1135.

(21) Wendt, R. A.; Mynott, R.; Hauschild, K.; Ruchatz, D.; Fink, G. *Macromol. Chem. Phys.* **1999**, *200*, 1340.

(22) Leclerc, M. K.; Waymouth, R. M. *Angew. Chem., Int. Ed.* **1998**, *37*, 922. (b) Fan, W.; Leclerc, M. K.; Waymouth, R. M. *J. Am. Chem. Soc.* **2001**, *123*, 9555.
(23) Arndt-Rosenau, M.; Beulich, I. *Macromolecules* **1999**, *32*, 7335.
(24) Bovey, F. A. *Polymer Conformation and Configuration*; Academic Press: New York, 1969.
(25) (a) Ham, G. E. In *Copolymerization*; Interscience Publishers: New York, 1964; p 1. (b) Odian, G. *Principles of Polymerizations,* 3rd ed.; Wiley & Sons: New York, 1991; p 455.
(26) Kaminsky, W.; Engehausen, R.; Kopf, J. *Angew. Chem., Int. Ed. Engl.* **1995**, *34*, 2273−2275.
(27) Kaminsky, W., private communication.
(28) We cannot exclude effects of small (±1−2 °C) local thermal excursions.
(29) Fink, G.; Herfert, N.; Montag, P. In *Ziegler Natta Catalysts;* Fink, G., Mülhaupt, Brintzinger, H. H., Eds.; Springer-Verlag: Berlin, 1995; p 159.
(30) Yoshida, Y.; Mohri, J.; Ishii, S.; Mitani, M.; Saito, J.; Matsui, S.; Makio, H.; Nakano, T.; Tanaka, H.; Onda, M.; Yamamoto, Y.; Mizuno, A.; Fujita, T. *J. Am. Chem. Soc.* **2004**, *126* 12023−12032.
(31) Brun, Y.; Nielson, R.; Tacconi, R. *Proc. Int. GPC Symp. 98, Phoenix, AZ* **1998***,* 415.

MA051682J